A Simple Parameterization of Land Surface Processes for Meteorological Models

J. NOILHAN AND S. PLANTON

Centre National de Recherches Météorologiques, Toulouse, France

ABSTRACT

A parameterization of land surface processes to be included in mesoscale and large-scale meteorological models is presented. The number of parameters has been reduced as much as possible, while attempting to preserve the representation of the physics which controls the energy and water budgets. We distinguish two main classes of parameters. The spatial distribution of primary parameters, i.e., the dominant types of soil and vegetation within each grid cell, can be specified from existing global datasets. The secondary parameters, describing the physical properties of each type of soil and vegetation, can be inferred from measurements or derived from numerical experiments. A single surface temperature is used to represent the surface energy balance of the land/cover system. The soil heat flux is linearly interpolated between its value over bare ground and a value of zero for complete shielding by the vegetation. The ground surface moisture equation includes the effect of gravity and the thermo–hydric coefficients of the equations have been either calculated or calibrated using textural dependent formulations. The calibration has been made using the results of a detailed soil model forced by prescribed atmospheric mean conditions. The results show that the coefficients of the surface soil moisture equation are greatly dependent upon the textural class of the soil, as well as upon its moisture content. The new scheme has been included in a one-dimensional model which allows a complete interaction between the surface and the atmosphere. Several simulations have been performed using data collected during HAPEX-MOBILHY. These first results show the ability of the parameterization to reproduce the components of the surface energy balance over a wide variety of surface conditions.

1. Introduction

During recent years, climate modelers have paid special attention to the processes coupling the soil surface and the atmosphere. Many sensitivity experiments, reviewed by Mintz (1981) and Rowntree (1983), have been performed with General Circulation Models (GCMs). These experiments involved changing the surface characteristics such as albedo, humidity, moisture availability or roughness. Generally, the chosen changes were in a large enough spectrum in order to obtain a statistically significant response and to explore the mechanisms involved, rather than to give a realistic reproduction of climatic changes. However, these simulations have shown a great interdependence between the climatic behavior of the atmosphere and the land surface processes.

At smaller scales, several experiments performed with 2D models (Ookouchi et al. 1984; Benjamin 1986; Mahfouf et al. 1987) and 3D models (McCumber 1980; Benjamin and Carlson 1986) have also shown the influence of the soil nature and of its vegetation coverage on the atmospheric circulation. McCumber (1980) has pointed out their effects on both strength and pattern

of the sea breeze convergence. Benjamin and Carlson (1986) and Benjamin (1986) have isolated the role of the differential surface heating combined with orography, on the outbreak of severe storms.

All these studies lead to the conclusion that, with both large-scale and mesoscale models, it is necessary to improve the representation of land surface processes. Deardorff (1978) has proposed a parameterization of heat and water exchanges at the land surface to be used in meteorological models. In his approach, he includes the representation of a vegetation layer with its canopy, interacting both with the soil surface and the atmosphere. This model has been followed by several parameterizations with various degrees of simplicity (Dickinson 1984; Sellers et al. 1986).

The present study is limited to the case of short-range simulations (a few days). Climatic simulations or long-range forecasting require modifications that will not be discussed here. Furthermore, we only consider snow-free land surfaces, excluding the case of frozen soils. The parameterization is guided by the concern to keep as low as possible the number of parameters describing the physics and to preserve the main mechanisms that control the energy and water balances at the surface. This scheme is to be used in numerical weather prediction models for which the analysis of surface fields, and more specifically of surface humidity, is of crucial importance; a large number of parameters

Corresponding author address: Dr. J. Noilhan, Direction de la Meteorologie Nationale, Centre National de Rescherches Météorologiques, 42, Avenue Coriolis, Toulouse, France.

is a destabilizing factor for the inverse methods needed in initialization. To represent the main processes at the land surface, observational data and one dimensional simulations suggest that we must first of all take into account the wide range of thermo–hydric properties of soils, depending upon their nature and their water content. It is also important to reproduce the low thermal inertia of vegetation and its ability to directly reevaporate intercepted rain water and dew, as well as to delay evaporation from the ground surface.

The next section of this paper defines the input parameters used in the land surface scheme. The model computes five prognostic variables: the surface temperature T_S, representative of both canopy and soil surface; the mean surface temperature T_2; the surface volumetric water content w_g; the mean volumetric water content w_2; the interception water store W_r for the canopy. The relevant governing equations are described in sections 3 to 6. In section 4, we give details about the particular procedure used to calibrate the coefficients of the soil water equations, over various soil types and wetness conditions. The first results obtained with a one-dimensional soil–atmosphere model including this scheme, using recently collected data during the HAPEX-MOBILHY experimental program (André et al. 1986), are presented in section 7.

2. The parameters

The parameters have been chosen in order to characterize the main physical processes, while attempting to reduce the number of independent variables. They can be divided into two categories: primary parameters needing to be specified by spatial distribution, and secondary parameters whose values can be associated with the values of the primary parameters (Table 1).

a. Primary parameters

These describe the nature of the land surface and its vegetation coverage by means of only two numerical indices: the dominant vegetation type and soil type within each grid cell. The vegetation type can be inferred from data bases recently developed for climatic purposes or from remote sensing observations. Its use in a model addresses the questions of the parameters that can be derived from its specification, and of the change of scale from the original datasets. The main drawback of the climatological classifications is that they are greatly dependent upon the parameters for which they have been constructed. It is the case for the global distribution of 35 vegetation types on a 2° by 2° grid, proposed by the CLIMAP group (1981) for albedo studies. A first attempt to give a sufficiently detailed classification to allow other parameters specifications has been made by Matthews (1983) using the UNESCO classification system. The original 178 types of natural vegetation, on a 1° by 1° grid, can be aggregated according to the study of a particular physical

process. Another dataset has been constructed by Wilson and Henderson-Sellers (1985, referred to hereafter as WHS) with the same resolution and 53 vegetation/land cover types. Here the different types have been determined on the basis of expected requirements in general circulation models. For classifications deduced from satellite observations, the question is their dependence upon the radiance measurements which include complex physical processes. For both kind of datasets, their use in a model generally requires degrading them to a coarser resolution. The methods discussed by Matthews (1983) and WHS involve an appropriate averaging procedure for each parameter, but the details are outside the scope of this paper.

The soil type is given in existing climatological datasets with the same difficulties than previously mentioned. For CLIMAP, only the reflectivity characteristics of the soil surface have been taken into account to determine classes, since they were defined for albedo studies. The soil types in WHS include information about the texture, the color and the drainage, resulting in 21 different groups. The texture specification is very important for our purpose as Cosby et al. (1984) have shown that it is critical to determine the hydraulic properties of soil. The three classes defined by WHS can be included in the classification of the US Department of Agriculture (USDA) for which we have adjusted the coefficients for our parameterization.

b. Secondary parameters

Secondary parameters describe a wide variety of physical characteristics of the soil and of the vegetation. Clapp and Hornberger (1978) and Cosby et al. (1984) have proposed a classification of hydraulic properties according to their texture. They retained the USDA 11 soil types, determined by their percentage of clay, silt and sand. All the physics of water transfer is described by means of five parameters: the saturated and wilting point volumetric moisture contents w_{sat} and w_{wilt} respectively, the saturated matric potential ψ_{sat}, the saturated hydraulic conductivity K_{sat}, and b, the slope of the retention curve on a logarithmic graph. Two formulaes relate the matric potential ψ and the hydraulic conductivity K, to the volumetric water content w:

$$\psi = \psi_{sat}(w_{sat}/w)^b \qquad (1)$$

$$K = K_{sat}(w/w_{sat})^{2b+3}. \qquad (2)$$

McCumber and Pielke (1981) give expressions relating thermal properties to the soil water content, depending upon the soil nature. The volumetric heat capacity c_g and the thermal conductivity λ vary with w and ψ through:

$$c_g = (1 - w_{sat})c_i + wc_{H_2O} \qquad (3)$$

$$\lambda = 418 \exp - (\log\psi + 2.7), \text{ if } \log|\psi| < 5.1 \quad (4a)$$

$$\lambda = 0.171 \text{ J s}^{-1} \text{ m}^{-1} \text{ K}^{-1}, \qquad \text{ if } \log|\psi| > 5.1 \quad (4b)$$

where c_i is the volumetric heat capacity for the solid fraction of soil and c_{H_2O} the one for water.

This set of thermo–hydric parameters has been used to calculate and adjust some parameters summarized in Table 1 ($C_{G_{sat}}$, C_{1sat}, C_{2ref}, a, p), by specific procedures discussed in sections 3 and 4.

The last soil parameter d_2 is related to the vegetation type, since it is defined as the depth at which the soil moisture flux becomes negligible for a period of about one week. Thus, d_2 is deeper than the root zone depth and controls the deep runoff.

The fraction of vegetation, denoted as veg, must be understood as a foliage shielding factor of the ground from solar radiation. It can be estimated with numerical simulations using the surface energy balance, as will be shown in section 7. At a regional scale, it seems likely that veg can be deduced from satellite observations, at least during the vegetation growth.

The surface resistance R_s is defined as the resistance to the transfer of water from the root zone to the leaf surfaces. It depends upon the formulation of transpiration, and in particular upon the definition of the surface temperature used to calculate the saturation specific humidity. When the soil is well supplied with water, the minimum surface resistance R_{smin} is related to the observed stomatal resistance of a given leaf. There are numerous measurements of stomatal resistances for different kinds of vegetation at different stages of their development (Szeicz and Long 1969; Monteith 1975, 1976). Either previous references or results from numerical simulations of the Bowen ratio (section 7), can be used to evaluate R_{smin}. The maximum surface resistance R_{smax} is arbitrarily set to 5000 s m^{-1}.

Values for the last four parameters—Leaf Area Index (LAI), roughness length Z_0, albedo α, and emissivity ϵ—can be deduced from the abovementioned classifications according to the dominant vegetation and soil types.

TABLE 1. Soil and vegetation parameters.

Primary parameters	
Dominant type of vegetation	
Dominant type of soil texture	
Secondary parameters	
Saturated volumetric moisture content	w_{sat}
Wilting point volumetric water content	w_{wilt}
Slope of the retention curve	b
Soil thermal coefficient at saturation	C_{Gsat}
Value of C_1 at saturation	C_{1sat}
Value of C_2 for $w_2 = 0.5w_{sat}$	C_{2ref}
Coefficients of w_{geq} formulation	a, p
Depth of the soil column	d_2
Fraction of vegetation	veg
Minimum surface resistance	R_{smin}
Leaf Area Index	LAI
Roughness length	z_0
Albedo	α
Emissivity	ϵ

3. Treatment of the soil heat content

The pronostic equations for the surface temperature T_S and for its mean value T_2 over one day τ, are obtained from the force restore method proposed by Bhumralkar (1975) and Blackadar (1976):

$$\frac{\partial T_s}{\partial t} = C_T G - \frac{2\pi}{\tau}(T_s - T_2) \qquad (5)$$

$$\frac{\partial T_2}{\partial t} = \frac{1}{\tau}(T_S - T_2). \qquad (6)$$

In Eq. (5), G is the heat storage rate in the soil–vegetation medium, which is equal to the sum of all the atmospheric fluxes at the surface:

$$G = R_n - H - \text{LE}, \qquad (7)$$

where R_n is the net radiation at the surface, and H and LE the sensible and latent heat fluxes from the atmosphere. The first term on the right-hand side of Eq. (5) represents the diurnal forcing of T_S by the heat flux G, and the second one tends to restore T_S to the mean soil temperature T_2.

The coefficient C_T is expressed by

$$C_T = 1 \Big/ \left(\frac{1 - \text{veg}}{C_G} + \frac{\text{veg}}{C_V}\right), \qquad (8)$$

where $C_V = 10^{-3}$ K m^2 J^{-1} and

$$C_G = 2\left(\frac{\pi}{\lambda c_g \tau}\right)^{1/2}. \qquad (9)$$

For bare ground conditions (i.e., veg = 0), the coefficient C_T equals C_G, and T_S can be calculated if we assume constant thermal properties of the soil and a sinusoidally varying value of the heat flux G. On the other hand, when the ground is totally shielded by vegetation (i.e., veg = 1), C_T tends towards C_V. Considering that the heat capacity of the vegetation is negligible, we take $C_V \gg C_G$. Then for complete shielding, the first term on the right side of Eq. (5) becomes larger than the restore term. Equation (5) is then reduced to $G = 0$ and T_S is obtained as the solution of the surface energy balance without any heat storage by plants. This method is similar to most other detailed land surface schemes, including a one-layer foliage parameterization (Deardorff 1978; Dickinson 1984). When the ground is partially covered by the vegetation, the expression for C_T combines C_V and C_G, allowing linearization of the heat flux within the soil/vegetation medium.

The soil properties in Eq. (9) depend upon both the soil texture and the soil moisture. The dependence of λ and c_g upon the soil type and the mean volumetric water content w_2 of the soil column are deduced from the expressions given by McCumber and Pielke (1981). We have adjusted a power law to the analytical expression for C_G given by Eqs. (3)–(4) and (9), as follows:

TABLE 2. Estimated and calibrated coefficients of the thermo-hydric equations; b is the slope of the retention curve given by Clapp and Hornberger (1978) for the 11 soil types of the USDA textural classification; C_{Gsat} is in K m^2 J^{-1} and all other coefficients are dimensionless.

Soil texture	b	C_{Gsat}	p	a	C_{2ref}	C_{1sat}
Sand	4.05	3.222	4	0.387	3.9	0.082
Loamy sand	4.38	3.057	4	0.404	3.7	0.098
Sandy loam	4.90	3.560	4	0.219	1.8	0.132
Silt loam	5.30	4.418	6	0.105	0.8	0.153
Loam	5.39	4.111	6	0.148	0.8	0.191
Sandy clay loam	7.12	3.670	6	0.135	0.8	0.213
Silty clay loam	7.75	3.593	8	0.127	0.4	0.385
Clay loam	8.52	3.995	10	0.084	0.6	0.227
Sandy clay	10.40	3.058	8	0.139	0.3	0.421
Silty clay	10.40	3.729	10	0.075	0.3	0.375
Clay	11.40	3.600	12	0.083	0.3	0.342

$$C_G = C_{Gsat}\left(\frac{w_{sat}}{w_2}\right)^{b/2\log 10}, \qquad (10)$$

where the exponent is derived from the analytical form, and C_{Gsat} is estimated for each soil texture (Table 2). In order to limit the values for dry conditions, C_G can-

not exceed a maximum given by (10) when w_2 equals the wilting point value w_{wilt}.

The resulting values of C_G are depicted in Fig. 1. The variations are given for a coarse, a medium and a fine soil texture versus the mean volumetric water content w_2. For a given w_2, the finest texture exhibits higher values of C_G because of the reduction of its thermal capacity. In Fig. 1, one can compare the analytical (dashed line) and adjusted curves in the case of loam.

4. Treatment of the soil water

The soil model considers the surface volumetric water content w_g representative of a thin layer (a few millimeters) interacting directly with the atmosphere, and the mean volumetric water content w_2 of a soil column of depth d_2 and of one square meter cross section (1 meter in the case of bare ground). Over the vegetation, we define a skin reservoir for the amount of liquid water W_r retained on the foliage per unit ground area.

a. Rate equations for w_g and w_2

Equations for w_g and w_2 are derived from the force restore method applied by Deardorff (1977) to the ground soil moisture:
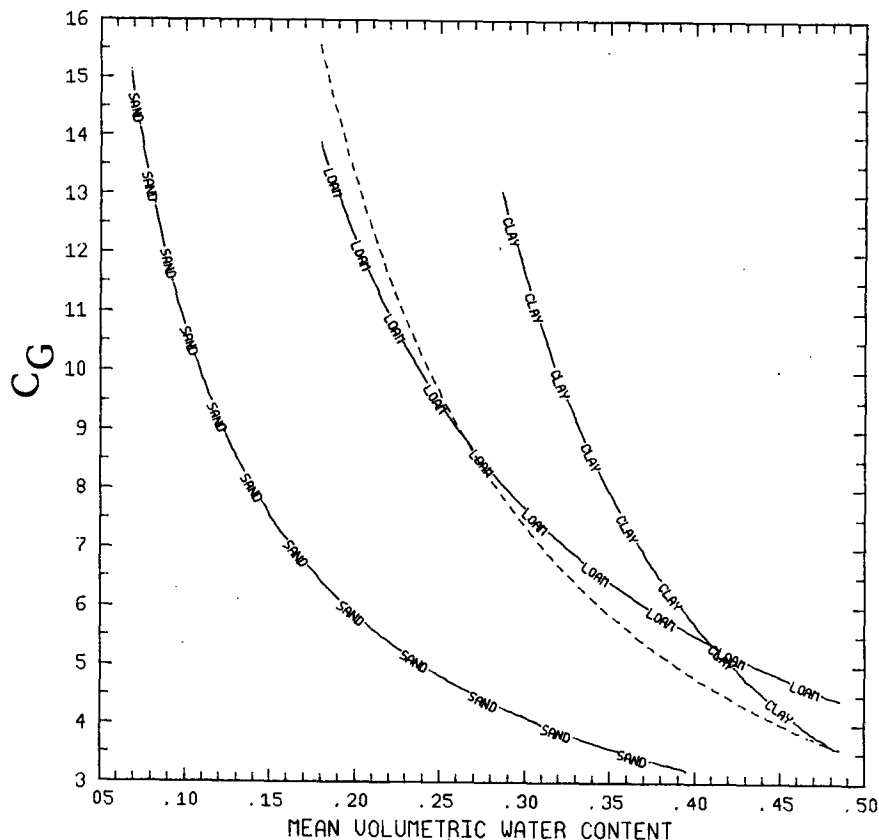

FIG. 1. Variations of C_G (in 10^6 K m^2 J^{-1}) versus w_2 given by Eq. (10), for sand, silt loam and clay; the dashed line corresponds to a calculation from thermal properties of McCumber and Pielke (1981) and hydraulic properties of Clapp and Hornberger (1978), in the case of silt loam.

$$\frac{\partial w_g}{\partial t} = \frac{C_1}{\rho_w d_1}(P_g - E_g) - \frac{C_2}{\tau}(w_g - w_{geq}),$$

$$0 \leqslant w_g \leqslant w_{sat} \quad (11)$$

$$\frac{\partial w_2}{\partial t} = \frac{1}{\rho_w d_2}(P_g - E_g - E_{tr}), \quad 0 < w_2 \leqslant w_{sat}, \quad (12)$$

where P_g is the flux of liquid water reaching the soil surface, E_g the evaporation at the soil surface, E_{tr} the transpiration rate, ρ_w the density of liquid water and d_1 an arbitrary normalization depth of 10 centimeters. The first term on the right hand side of Eq. (11) represents the influence of surface atmospheric fluxes where the contribution of the water extraction by the roots is neglected. The second term characterizes the diffusivity of water in the soil. The two coefficients C_1 and C_2, and the surface volumetric moisture w_{geq} when gravity balances the capillarity forces, have been calibrated for different soil textures and soil moistures as discussed below.

Equation (12) represents the water budget over the soil layer of depth d_2. For a short length of time (a few days), we neglect the drainage at the bottom of the layer. All the transpiration is extracted from this layer, since it includes the rooting zone.

Runoff occurs when w_g or w_2 exceeds the saturation value w_{sat}. This occurs either when the total soil layer becomes saturated ($w_2 = w_{sat}$), or when the intensity of precipitation is sufficiently greater than the infiltration rate to allow w_g to reach w_{sat}.

b. Determination of w_{geq}

In the restore term of Eq. (12) of Deardorff (1978), gravity was not taken into account. In this case w_{geq} in Eq. (11) would be equal to w_2. However, we see in Fig. 2 that, particularly in the case of sand, the equilibrium values can become notably lower than the mean moisture. The values of w_{geq} versus w_2 have been calculated using Clapp and Hornberger's (1978) specifications for hydraulic properties, and the condition of balance between capillarity and gravity forces in the unsaturated case:

$$\frac{\partial \psi}{\partial z} = 1. \quad (13)$$

When saturation occurs, ψ is limited to the maximum value ψ_{sat}. We have adjusted a polynomial function to the points (w_{geq}, w_2):

$$y = x - ax^p(1 - x^{8p}), \quad (14)$$

where $x = w_2/w_{sat}$ and $y = w_{geq}/w_{sat}$; the two parameters a and p (integer) have been calculated for all the soil types (Table 2). The result of this adjustment is given in Fig. 2 for sand, silt loam and clay, with the exact solution in the case of silt loam (dashed line).

c. Calibration of C_1 and C_2

These two dimensionless coefficients are highly dependent upon both the soil moisture content and the soil texture. Unfortunately, to the best of our knowledge, the only parameterization of C_1 and C_2 has been derived by Deardorff (1977) from the data of Jackson (1973) that are restricted to only one kind of soil (Adelanto loam). Thus, in order to parameterize C_1 and C_2 for a wide variety of soil conditions, we have used a detailed multilayer one-dimensional model.

This Reference Model (RM) has 26 layers and resolves temperature and water profiles by Fourier and Darcy equations (Noilhan 1987). Vapor transfers are neglected, and only bare ground conditions are considered here. The levels are irregularly spaced with higher resolution near the surface, and the hydraulic properties are taken from Clapp and Hornberger (1978). In the experiments described below, RM is forced by prescribed atmospheric mean conditions, i.e., incoming radiation, wind speed, specific humidity and temperature at 2 m.

The coefficient C_2 characterizes the velocity at which the water profile is restored to its equilibrium. It increases with hydraulic conductivity. To obtain an estimate, we have integrated RM with the boundary conditions:

$$W(0) = P_g - E_g = 0 \quad (15a)$$

$$W(d_2) = \rho_w K \left(\frac{\partial \psi}{\partial z} - 1 \right)\bigg|_{d_2} = 0, \quad (15b)$$

where $W(z)$ is the water flux at depth z. This condition requires that the total water content of the soil column is conserved, as long as no saturation occurs along the water profile (no runoff). If the evolution of w_g is described by (11) and (15), then at a given time t:

$$(w_g - w_{geq})(t) = (w_g - w_{geq})(t_0)e^{-C_2(t-t_0)/\tau}. \quad (16)$$

Thus, C_2 can be calculated with these assumptions from the RM results:

$$C_2 = \frac{\tau}{t_1 - t_0}, \quad (17)$$

where $t_1 - t_0$ is the e-folding time of the departure ($w_g - w_{geq}$) from its initial value at time t_0. This estimation has been performed starting from different water profiles, differing in total water content as well as in profile shape. The results suggest mainly a dependence of C_2 upon w_2; we propose:

$$C_2 = C_{2ref}\left(\frac{w_2}{w_{sat} - w_2 + w_l}\right), \quad (18)$$

where w_l is a small numerical value which limits C_2 at saturation. The coefficient C_{2ref} has been estimated from the mean value of C_2 at a given w_2 with different initial profiles (Table 2). We have represented in Fig. 3, for the cases of sand, silt loam and clay, the values
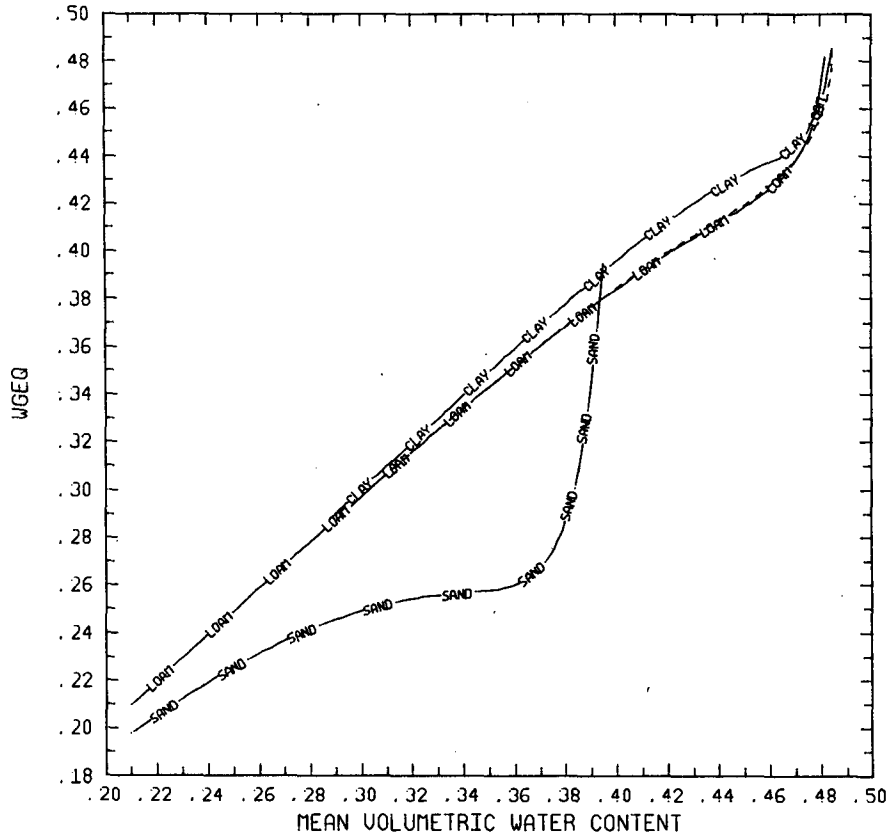
FIG. 2. Variations of w_{geq} (in m^3 m^{-3}) versus w_2 given by Eq. (14), for sand, silt loam and clay; the dashed line corresponds to the exact calculation from Eq. (13) and hydraulic properties of Clapp and Hornberger (1978), in the case of silt loam.

of C_2 given by (18) and by RM versus w_2. It is important to mention that this method is less accurate when it is applied to extreme conditions. In the case of very dry soils, the slowness of transfers would induce very long integrations of RM. On the other hand, RM neglects vapor exchanges which become important for very dry soils. Near saturation, expression (1) is questionable, as has been pointed out by Clapp and Hornberger (1978).

The coefficient C_1 can be calculated assuming constant hydraulic properties in the soil and a sine variation of the surface water flux (Appendix). The solution of Darcy's law gives

$$C_1 = \frac{2d_1}{d} = C_{1sat}\left(\frac{w_{sat}}{w_g}\right)^{b/2+1} \quad (19)$$

$$d = \left(\frac{K\tau}{\pi c_w}\right)^{1/2}, \quad (20)$$

where d is the real depth to which the diurnal cycle extends, and c_w is the hydraulic capacity deduced from (1) by

$$c_w = \frac{\partial w}{\partial \psi}. \quad (21)$$

The coefficient C_{1sat} (Table 2), is calculated from the values of hydraulic parameters at saturation (A5).

Alternatively, C_1 can be estimated by integrating RM with the above mentioned atmospheric forcing and the boundary condition (15b).

If we suppose that w_g is solution of Eq. (11) and C_1 constant over the time interval $[t, t + \delta t]$, then:

$$C_1 = \frac{\rho_w d_1}{\int_t^{t+\delta t} E_g du}\left[\underbrace{w_g(t) - w_g(t + \delta t)}_{(a)}\right.$$
$$\left. - \underbrace{\frac{C_2}{\tau}\int_t^{t+\delta t}(w_g - w_{geq})(u)du}_{(b)}\right], \quad (22)$$

where C_2 and w_{geq} are given by the parameterizations (14) and (18). We have chosen t equal to one hour and deduced C_1, taking into account only the cases where the term (a) is at least ten times higher than (b) in order to limit the influence of the parameterizations of C_2 and w_{geq}. We start the integrations with homogeneous profiles of different mean water contents w_2. We have displayed in Fig. 4, for the three main textures, the points (C_1, w_g) and the analytical expression of C_1 versus w_g derived from (1)–(2) and (19)–(21). The
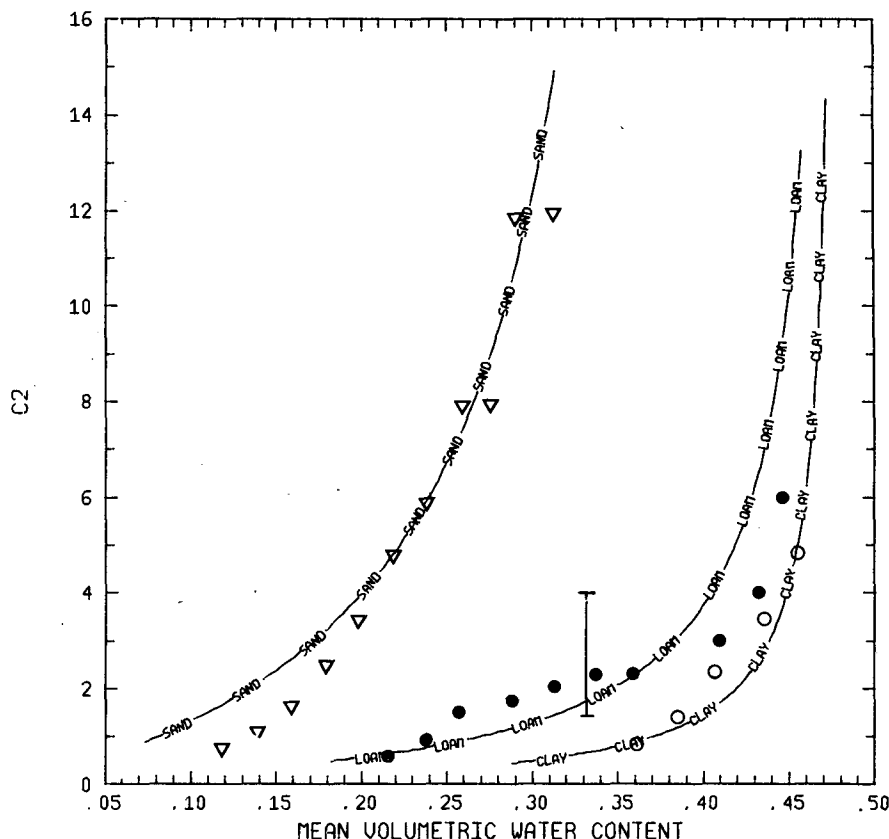
FIG. 3. Variations of the dimensionless coefficient C_2 versus w_2 given by Eq. (18), for the three main textures; the dots correspond to results given by the Reference Model (RM), in the case of sand (∇), silt loam ($\bullet$) and clay ($\bigcirc$); the error bar corresponds to different initializations of RM and is only indicative.

coefficient C_1 increases when the soil is drying since the hydraulic diffusivity is reduced. One can see that the numerical estimates are close to the analytic expression, an agreement that has been verified for different atmospheric forcings. This suggests that C_1 is mainly a function of hydraulic properties of the soil near the surface, and that, for an estimate, the homogeneity hypothesis is sufficient.

This is not the case for C_2 and w_{geq}, since the analytic calculation only indicates that C_2 must decrease when the texture becomes coarser (A6), and that w_{geq} must be reduced to represent gravity effects (A7). We have limited C_1 to the value given by (A5) for w_g equal to w_{wilt}.

5. Treatment of intercepted water

Rainfall and dew intercepted by the foliage feed a reservoir of water content W_r. This amount of water evaporates in the air at a potential rate from the fraction δ of the foliage covered with a film of water, as the remaining part $(1 - \delta)$ of the leaves transpires. Following Deardorff (1978), we set

$$\frac{\partial W_r}{\partial t} = \text{veg}P - (E_v - E_{tr}) - R_r, \qquad (23)$$

where P is the precipitation rate at the top of the vegetation, E_v the evaporation from the vegetation including the transpiration E_{tr} and the direct evaporation E_r when positive, and the dew flux when negative (in this case $E_{tr} = 0$), R_r is the runoff of the interception reservoir. This runoff occurs when W_r exceeds a maximum value W_{rmax} depending upon the density of the canopy, i.e., roughly proportional to vegLAI. According to Dickinson (1984), we use the simple equation:

$$W_{rmax} = 0.2 \text{ vegLAI [mm]}. \qquad (24)$$

6. The surface fluxes

As previously noted, we consider only one energy balance for the whole system ground–vegetation. As a result, heat and mass transfers between the surface and the atmosphere are related to the mean values T_S and w_g.
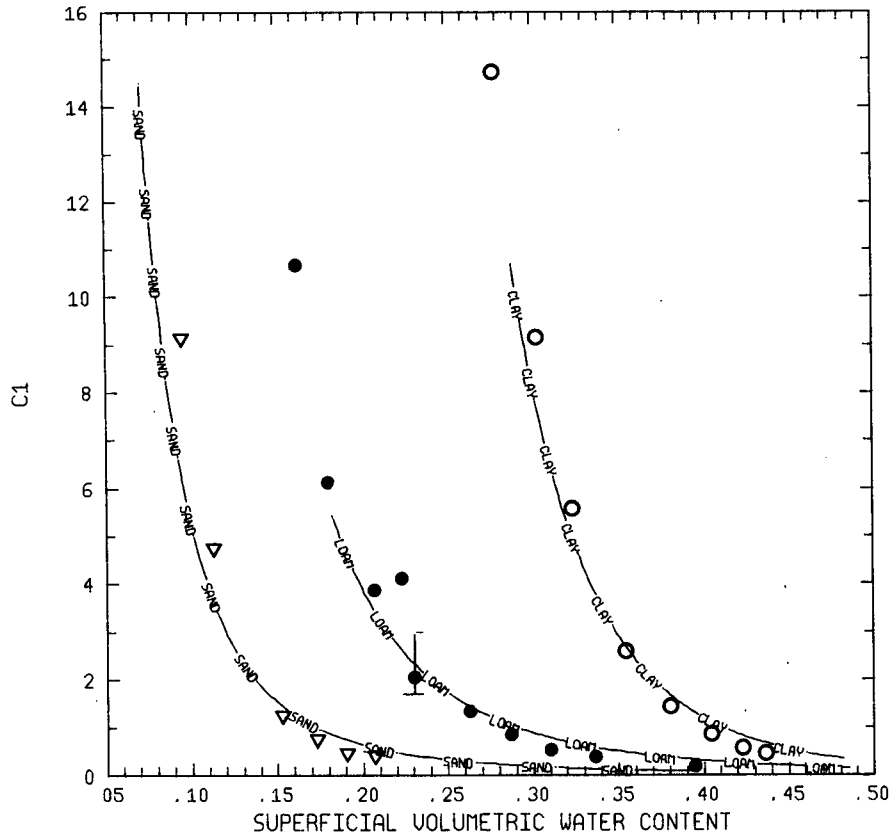
FIG. 4. As in Fig. 3 but for C_1 versus w_g given by Eq. (19).

The net radiation at the surface is the sum of the absorbed fractions of the incoming solar radiation R_G and of the atmospheric infrared radiation R_A, reduced by the emitted infrared radiation:

$$R_n = R_G(1 - \alpha) + \epsilon(R_A - \sigma T_S^4), \qquad (25)$$

where the albedo α and the emissivity ϵ combine linearly the soil and the vegetation reflectivities; and σ is the Stefan–Boltzmann constant.

The turbulent fluxes are calculated by means of the classical aerodynamic formulaes. For the sensible heat flux:

$$H = \rho_a c_p C_H V_a (T_S - T_a), \qquad (26)$$

where c_p is the specific heat; ρ_a, V_a and T_a are respectively the air density, the wind speed and the temperature at an atmospheric level z_a; C_H is the drag coefficient depending upon the thermal stability of the atmosphere.

The water vapor flux E is the sum of the evaporation E_g from the soil surface and of the evapotranspiration E_v from the vegetation, we set

$$E_g = (1 - \text{veg})\rho_a C_H V_a (h_u q_{\text{sat}}(T_s) - q_a)$$

$$E_v = \text{veg}\,\rho_a C_H V_a h_v (q_{\text{sat}}(T_s) - q_a), \qquad (27)$$

where $q_{\text{sat}}(T_S)$ is the saturated specific humidity at the temperature T_S and q_a the atmospheric specific humidity at the level z_a.

The relative humidity h_u at the ground surface is related to the superficial soil moisture w_g. Several experiments have shown that the surface evaporates at the potential rate when the soil moisture exceeds the so-called "field capacity" w_{fl}, often taken equal to $0.75 w_{\text{sat}}$; we assume:

$$h_u = \frac{1}{2}\left[1 - \cos\left(\frac{w_g}{w_{fl}}\pi\right)\right], \quad \text{if} \quad w_g < w_{fl}$$

$$h_u = 1, \qquad\qquad\qquad\quad \text{if} \quad w_g \geqslant w_{fl}. \quad (28)$$

When the flux E_v is positive, the Halstead coefficient h_v takes into account the direct evaporation E_r from the fraction δ of the foliage covered by intercepted water, as well as the transpiration E_{tr} of the remaining part of the leaves:

$$h_v = (1 - \delta)R_a/(R_a + R_s) + \delta \qquad (29)$$

$$E_r = \text{veg}\,\frac{\delta}{R_a}(q_{\text{sat}}(T_S) - q_a) \qquad (30)$$

$$E_{\text{tr}} = \text{veg}\,\frac{1 - \delta}{R_a + R_s}(q_{\text{sat}}(T_S) - q_a). \qquad (31)$$

When E_v is negative, the dew flux is supposed to occur at the potential rate, and h_v is taken equal to 1.

Following Deardorff (1978), δ is a power function of the moisture content of the interception reservoir:

$$\delta = \left(\frac{W_r}{W_{r\max}} \right)^{2/3}. \tag{32}$$

In expressions (29–31), the aerodynamic resistance R_a is equal to $1/(C_H V_a)$. The surface resistance R_s depends both upon atmospheric factors and upon available water in the soil; it is given by:

$$R_s = \frac{R_{s\min}}{\text{LAI}} F_1 F_2^{-1} F_3^{-1} F_4^{-4}. \tag{33}$$

The factor F_1 measures the influence of the photosynthetically active radiation (Sellers et al. 1986), and is assumed to be equal to $0.55 R_G$; from Dickinson (1984), we set

$$F_1 = \frac{1 + f}{f + R_{s\min}/R_{s\max}}$$

with

$$f = 0.55 \frac{R_G}{R_{GL}} \frac{2}{\text{LAI}}, \tag{34}$$

where R_{GL} is a limit value of 30 W m^{-2} for a forest and of 100 W m^{-2} for a crop.

The factor F_2 takes into account the effect of the water stress on the surface resistance; it varies between 0 and 1 when w_2 varies between w_{wilt} and a critical value w_{cr} of $0.75 w_{\text{sat}}$ (Thompson et al. 1981):

$$F_2 = \begin{cases} 1, & \text{if } w_2 > w_{\text{cr}} \\ \dfrac{w_2 - w_{\text{wilt}}}{w_{\text{cr}} - w_{\text{wilt}}}, & \text{if } w_{\text{wilt}} \leqslant w_2 \leqslant w_{\text{cr}} \\ 0, & \text{if } w_2 < w_{\text{wilt}}. \end{cases} \tag{35}$$

The factor F_3 represents the effects of vapor pressure deficit of the atmosphere. This has been already demonstrated by Jarvis (1976) for coniferous and reproduced by Sellers et al. (1986):

$$F_3 = 1 - g(e_{\text{sat}}(T_S) - e_a), \tag{36}$$

where g is a species-dependent empirical parameter.

We have derived a value of 0.025 H pa^{-1} for a coniferous forest from the HAPEX-MOBILHY dataset.

The factor F_4 introduces an air temperature dependence on the surface resistance. Following Dickinson (1984), we set

$$F_4 = 1.0 - 0.0016(298.0 - T_a)^2. \tag{37}$$

7. First results

We describe here some results obtained in one dimensional simulations, coupling the soil/vegetation scheme to an atmospheric model. The data used are derived from the HAPEX-MOBILHY experiment (HM), that took place in southwestern France during 1985 and 1986 (André et al. 1986).

a. The data

The main thrust of HM was to study evaporation processes over land at a General Circulation Model grid scale, i.e., 100 km by 100 km. This observational program also involved surface networks and remote sensing measurements. During a Special Observation Period (SOP), a wide range of instruments were deployed, among which were micrometeorological networks, well-suited for local water balance monitoring (André et al. 1988).

For a dozen selected sites, soil moisture has been measured every week to a depth of one meter. The so-called SAMER stations ("Système Automatique de Mesure de l'Evapotranspiration Régionale"), measured the four components of the radiation flux and the sensible heat flux together with the heat flux into the ground. The sensible heat flux is estimated from 15 min averaged gradients of wind and temperature, and the latent heat flux inferred by balancing the heat budget at the surface. The SAMER stations also measured 2 meters above the ground wind, temperature and relative humidity. The canopy parameters for the most significant vegetation covers (corn and forest) have also been estimated; this is the case, for example, for the LAI, vegetation height variations and albedo.

b. The model and the experiments

We have attempted to reproduce six observed surface energy balances over different types of soil and of vegetation at different stages of their development, corresponding to some SAMER stations locations (Table 3). Each experiment consists of a one day integration starting at 0000 UTC with clear sky conditions. The atmospheric model is the mesoscale prediction model of the French Weather Service (Bougeault 1986), limited here to the vertical dimension with 15 levels irregularly spaced. It includes a representation of the main physical processes, such as radiation, turbulent diffusion, and large-scale and convective precipitation.

The atmospheric transmissivities have been adjusted in order to nearly reproduce the observed global radiation at the top of the vegetation. All the simulations have been performed with forcing conditions for the advective terms, derived from interpolated analyses of atmospheric parameters over the HM area and given every 6 hours (Mercusot et al. 1987). The same analyses have been used to initialize the pressure, temperature, specific humidity and wind profiles of the atmosphere, as well as the soil temperatures, which were taken equal to the lower level atmospheric temperature. The initial soil water contents w_g and w_2 correspond to the averages of neutron sounding measurements over

TABLE 3. Initial soil moistures and parameters for 6 one-dimensional simulations with the land surface scheme; the date and the site refer to the HAPEX-MOBILHY dataset.

Case	Day	Site	Soil	Vegetation	Wg $(m^3 \, m^{-3})$	w_2 $(m^3 \, m^{-3})$	z_0 (m)	α	LAI $(m^2 \, m^{-2})$	R_{smin} (sm^{-1})	veg
1	06–16	Lubbon 2	Sand	Maïze	0.17	0.17	0.10	0.15	2.0	40	0.80
2	06–16	Caumont	Loam	Soja	0.26	0.26	0.02	0.24	1.0	40	0.70
3	06–16	Castelnau	Loam	Maïze	0.18	0.25	0.02	0.25	0.3	40	0.40
4	06–16	Estampon	Sand	Forest	0.14	0.20	1.00	0.10	2.3	100	0.99
5	07–10	Castelnau	Loam	Maïze ·	0.15	0.23	0.10	0.22	2.0	40	0.70
6	07–10	Lubbon 1	Sand	Oats	0.10	0.14	0.15	0.21	3.0	450	0.90

the first 0.1 and 1 m depth respectively. Additional measurements of the surface moisture using gypsum blocs have been used at some sites (cases 3 and 5).

All the parameters that can be inferred from observations have been specified (Table 3). This is the case for the soil texture, the albedo and LAI, which have been determined for each site. The roughness length has been taken equal to one tenth of the vegetation height. The minimum surface resistance R_{smin} has been deduced following Monteith (1976), and the emissivity ϵ has been set to 0.95. The values of the fraction of vegetation veg have been adjusted mainly to reproduce the soil surface heat flux since the heat storage in the vegetation layer has been neglected. The results obtained agree reasonably with the aspect of the land surface vegetation coverage.

c. Results

Figures 5 to 10 show the six daily variations of the observed (a) and modeled (b) components of the surface energy balance.

Cases 1 and 2 (Figs. 5 and 6) correspond to crop during the growing season when soils are well supplied with water. In both cases, the simulated and observed courses of net radiation R_n, soil heat flux G and turbulent fluxes H and LE are generally in good agreement. Particularly for case 1 (corn over sand), the time lag between the maximum values of H and LE is well predicted. In these cases, the calculated values of G are small (maximum of 25 W m^{-2}) and LE is the dominant turbulent flux, since the Bowen ratio at noon equals 0.53 and 0.35 for cases 1 and 2, respectively. In addition, surface evaporation is not intense, and E is mainly supplied by the transpiration E_v. For instance, the ratio of the mean daily values of E_v and E is equal to 0.65 for case 2.

Case 3 (Fig. 7) illustrates an example with a significant fraction of bare ground (veg = 0.4). The corn was 0.2 m high. We observe high values of G, reaching some 100 W m^{-2} at noon, since the amount of solar radiation at the ground surface was important. The model predicts the observed daily variations of G reasonably well. The magnitude and the diurnal variations of LE and H are also correctly simulated. In opposition to cases 1 and 2, the larger contribution to E is from

the surface evaporation E_g. The model results are thus, highly sensitive to the initial value of w_g. Total evaporation E reaches its maximum earlier in the day and then starts to decrease regularly. Such a latent heat daily variation is commonly observed over bare ground.

Turbulent fluxes for case 4 (Fig. 8) have been measured 5 meters above the forest and so represent the whole contribution of the surface and canopy exchanges. At this season, the ground surface was completely covered by the sublayer vegetation (brackens) and G was negligible. Consequently, we assume a value of veg close to one, prescribing the net radiation to be entirely balanced by turbulent fluxes. The resistance R_s increases during the day because of its dependence upon the vapor pressure deficit of the atmosphere, and so E is limited around noon. The simulation is in broad agreement with the observation, using a value of R_{smin} equal to 100 s m^{-1} representative of the entire vegetative cover (forest and brackens).

The last two cases correspond to a sunny day at the end of the SOP. Case 5 (Fig. 9) refers to the same site as case 3, but the corn was higher (height about 1 m). As a result, the values of both LAI and veg increase significantly (see Table 3). In opposition to case 3, E_v was the dominant exchange, inducing the decrease of the Bowen ratio.

The last case 6 (Fig. 10) corresponds to a field of mature oats. The sandy soil became dry ($w_g = 0.14$ m^3 m^{-3}). From measurements, its appears that transpiration was very low (maximum value of 100 W m^{-2}) and H very high, reaching 400 W m^{-2} at noon. The simulated evaporation is underestimated during the morning, probably because of an underprediction of dew. However, we note a general agreement with the observation obtained with R_{smin} equal to 450 s m^{-1}. This high value seems reasonable since, as maturation and senescence proceed, R_{smin} must increase from its minimum value (40 s m^{-1}). Similar seasonal evolution for cereals has been already described by Thompson et al. (1981).

8. Summary and conclusion

We propose a simple parameterization of land surface processes for mesoscale and general circulation
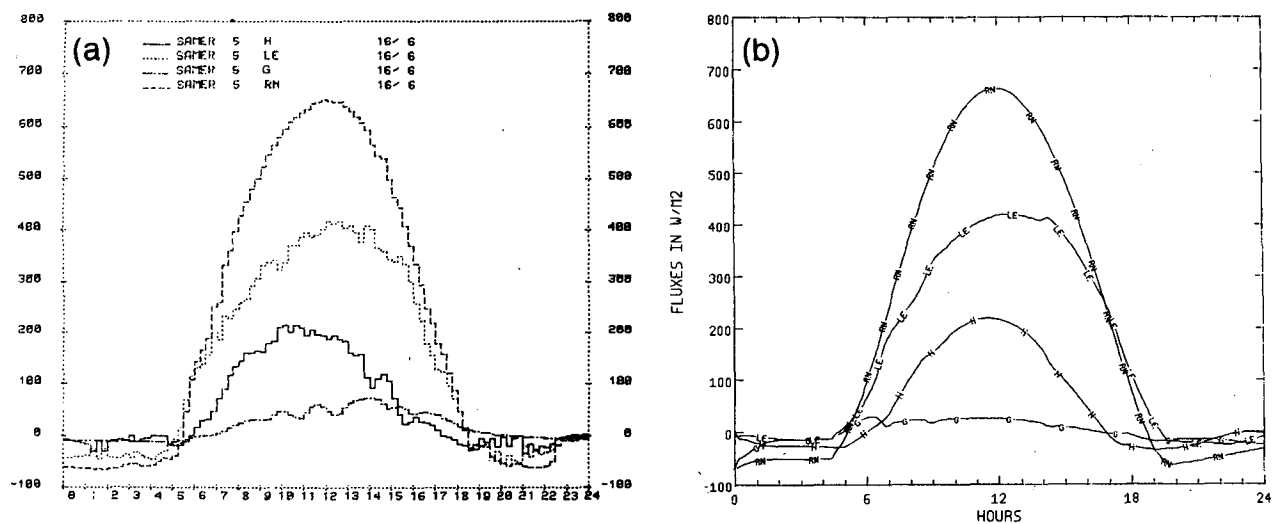
FIG. 5. Diurnal variations of observed (a) and simulated (b) surface fluxes (in W m^{-2}) for case 1 (Table 3): net radiation R_n, latent heat flux LE, sensible heat flux H and soil heat flux G.
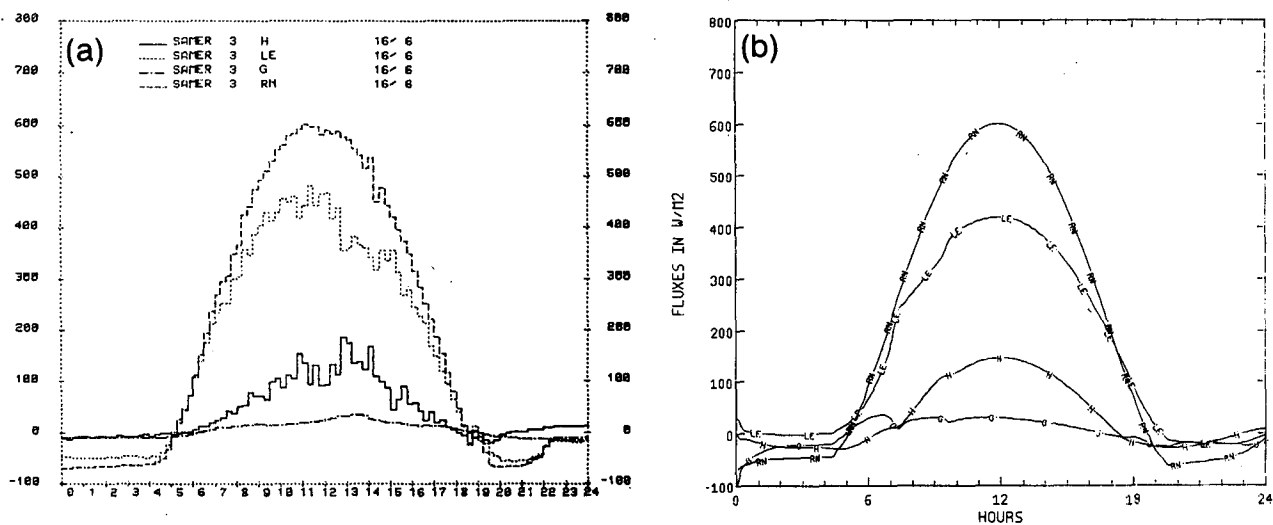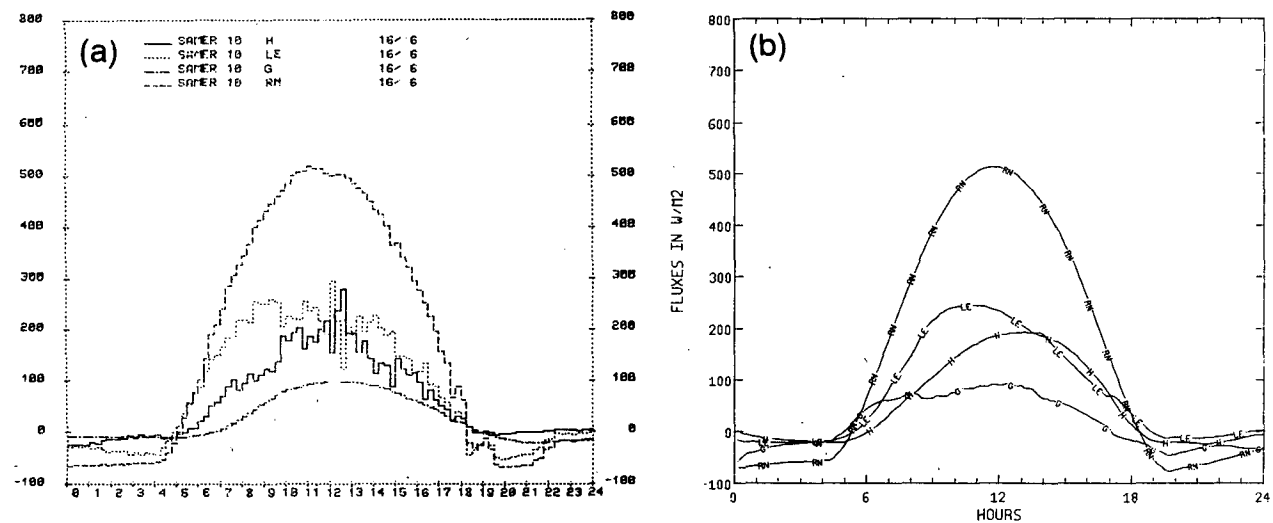

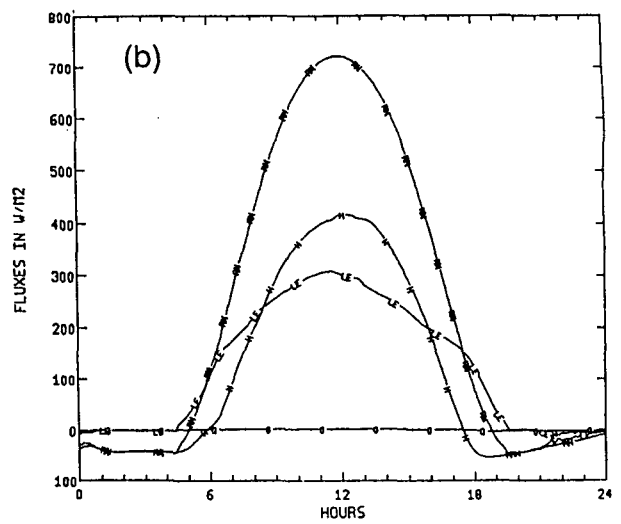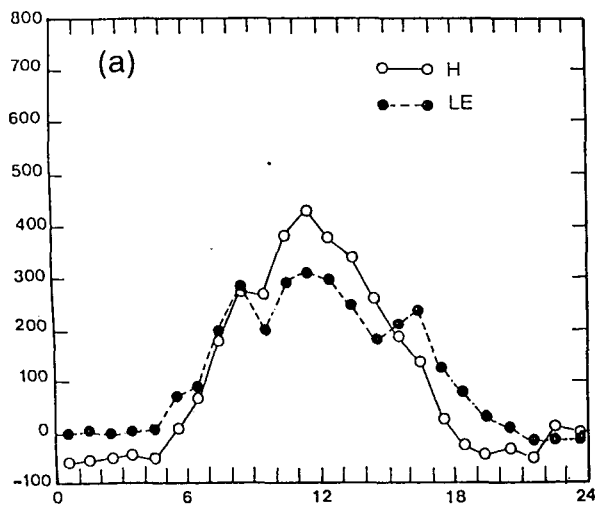FIG. 6. As in Fig. 5 but for case 2.

FIG. 7. As in Fig. 5 but for case 3.
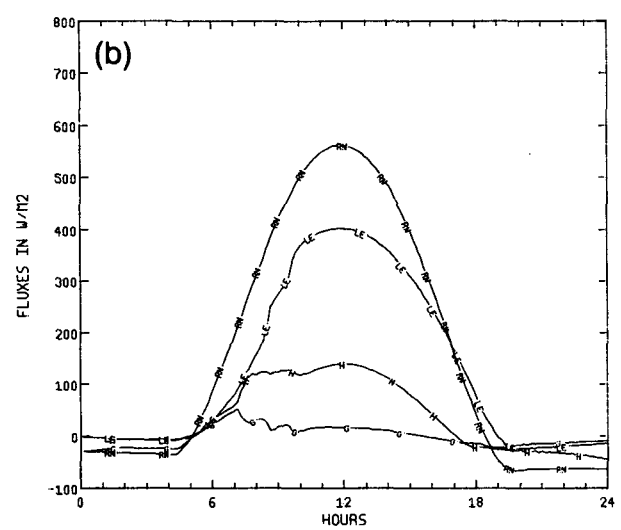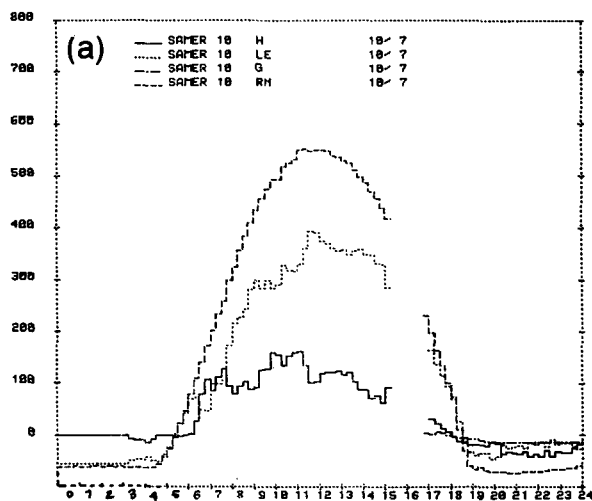
FIG. 8. As in Fig. 5 but for case 4.
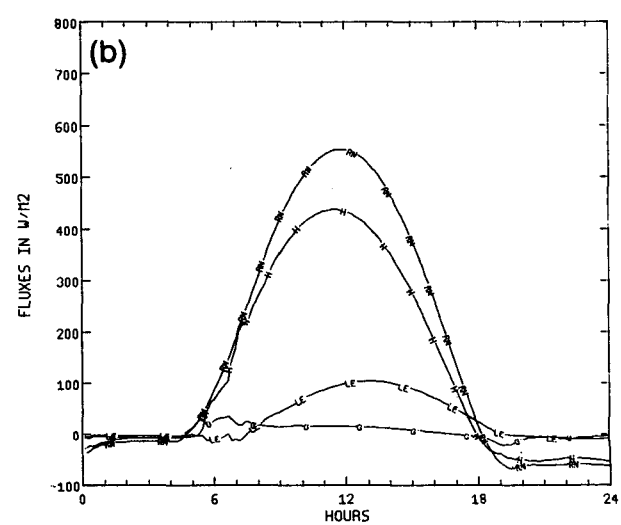

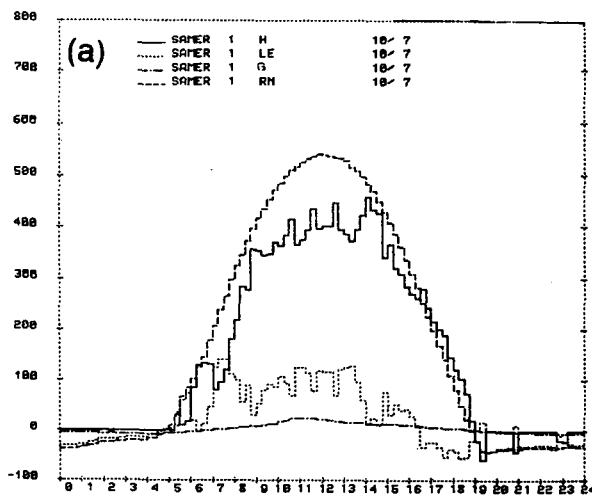FIG. 9. As in Fig. 5 but for case 5.

FIG. 10. As in Fig. 5 but for case 6.

models. This scheme has been designed for the best trade-off possible between accurate description of the main physical processes and restricting the number of parameters to be prescribed. One of the objectives is to describe the vegetation as simply as possible: a surface resistance controls the transpiration; the plants intercept precipitation and dew which evaporate at the potential rate; and the magnitude of the soil heat flux is modulated by the fraction of surface covered by vegetation. Additionaly, only one surface temperature is used to describe the entire energy exchange at the land/cover surface. Within the ground, heat and water transfers are dependent upon the soil texture and the water content. The water changes are calculated for both an upper thin layer and a deeper one at a rate derived from Deardorff's (1977) force restore method. A major difference from Deardorff's proposal is the inclusion of gravity effects in the restore term of the surface volumetric water content equation. Another one is the calibration of the coefficients of this equation upon the types and wetness of soils.

This calibration has been performed using the results of a detailed one-dimensional model as a reference, together with the formulations of Clapp and Hornberger (1978) for the hydraulic properties of soils associated with the USDA textural classification. The results show a great variability of the coefficients with the soil type and its moisture content.

The scheme requires the specification of two basic parameters which have a spatial distribution, i.e., the dominant types of soil and vegetation within each grid cell. These parameters may be obtained in principle by remote sensing or from existing datasets. They generate a set of secondary parameters which characterize a given soil texture or vegetal specy: thermal and hydraulic properties of the soil, and morphological and physiological properties of the vegetation. Most of these secondary parameters can be estimated by numerical and field experiments, or more simply, can be associated with the above mentioned datasets. Recent studies also show that some of them (veg, R_s) can be inferred from satellite observations (Tucker and Sellers 1986).

Preliminary results obtained with a one-dimensional version of the French Weather Service mesoscale model, incorporating our parameterization are presented, using data collected during HAPEX-MOBILHY. These tests correspond to clear sky conditions and are applied to various soil textures and vegetation covers at different stages of their development. The scheme, fully interactive with the boundary layer, reproduces well the observed variations of the components of the surface energy balance.

The parameterization is now being applied to a larger variety of surface and atmospheric conditions (rainy events) and to longer time periods (several weeks), in order to examine the realism of significant changes of the soil water content.

The next step will be the inclusion of the land surface scheme in the mesoscale model, adressing the important question of grid averaging process. The influence of subgrid variability on the surface fluxes, highly nonlinear dependent on the surface characteristics, has been already investigated by several authors (Mahrt 1987; Wetzel and Chang 1988). The HAPEX MOBILHY experiment provides a fruitful dataset at different scales to test assumptions related to spatial averaging at a grid scale. The results of these numerical experiments will be presented in a forthcoming paper.

APPENDIX

Analytical Estimation of C_1

If we assume that the soil hydric properties are homogeneous, we can describe the time evolution of w_g by an equation similar to the one introduced by Bhumralkar (1975) and Blackadar (1976) for the surface temperature. In this case, the matric potential obeys the diffusion equation:

$$\frac{\partial \psi}{\partial t} = \frac{K}{|c_w|} \frac{\partial^2 \psi}{\partial z^2}. \qquad (A1)$$

For a sinusoidal surface water flux with one day period, an exact solution of (A1) is:

$$\psi(z, t) = \bar{\psi}(z) + \Delta\psi \exp^{-z/d} \sin(\omega t - z/d), \qquad (A2)$$

where d is the depth reached by the diurnal wave ($d = \sqrt{2K/\omega|c_w|}$), the frequency ($\omega = 2\pi/\tau$) and $\bar{\psi}(z)$ a linear function of z. The surface matric potential ψ_0 is thus solution of

$$\frac{\partial \psi_0}{\partial t} = -\frac{\omega d}{\rho_w K} W_0 - \omega(\psi_0 - \bar{\psi}_0) + \omega d\left(\frac{d\bar{\psi}}{dz}(0) - 1\right), \qquad (A3)$$

where $\bar{\psi}_0 = \bar{\psi}(0)$ and W_0 is the surface water flux. Using (1)-(2) and (21), and making the additional hypothesis of an homogeneous mean profile [constant $\bar{\psi}(z)$], this leads to an equation satisfied by w_g:

$$\frac{\partial w_g}{\partial t} = \frac{2}{\rho_w d} W_0 - \frac{2\pi}{\tau b}\left(w_g - \bar{\psi}_0 \frac{w_g}{\psi_0} + d\frac{w_g}{\psi_0}\right) \qquad (A4)$$

that can be identified with Eq. (11); thus:

$$C_1 = \frac{2d_1}{d} = C_{1\text{sat}}\left(\frac{w_{\text{sat}}}{w_g}\right)^{b/2+1}$$

$$C_{1\mathrm{sat}} = 2\sqrt{\pi}\, d_1 \sqrt{w_{\mathrm{sat}}/b}\, |\psi_{\mathrm{sat}}|\, K_{\mathrm{sat}}\tau \qquad \text{(A5)}$$

$$C_2 = \frac{2\pi}{b} \qquad \text{(A6)}$$

$$w_{\mathrm{geq}} = \frac{w_g}{\psi_0}(\bar{\psi}_0 - d). \qquad \text{(A7)}$$

REFERENCES

André, J. C., J. P. Goutorbe and A. Perrier, 1986: HAPEX-MOB-ILHY: A hydrological atmospheric experiment for the study of water budget and evaporation flux at the climatic scale. *Bull. Meteor. Soc.,* **67,** 138–144.

——, and collaborators, 1988: HAPEX-MOBILHY: First results from the Special Observing Period. *Ann. Geophys.,* **6,** 477–492.

Benjamin, S. G., 1986: Some effects of surface heating and topography on the regional severe storm environment. Part. II: Idealized two dimensional experiments. *Mon. Wea. Rev.,* **114,** 330–343.

——, and T. N. Carlson, 1986: Some effects of surface heating and topography on the regional severe storm environment. Part I: 3-D simulations. *Mon. Wea. Rev.,* **114,** 307–329.

Bhumralkar, C. M., 1975: Numerical experiments on the computation of ground surface temperature in an atmospheric general circulation model. *J. Appl. Meteor.,* **14,** 67–100.

Blackadar, A. K., 1976: Modeling the nocturnal boundary layer. *Proc. Third Symp. on Atmospheric Turbulence, Diffusion and Air Quality,* Boston, Amer. Meteor. Soc., 46–49.

Bougeault, P., 1986: Le modéle Péridot: Une étude de qualification a méso-échelle (The French weather service limited area model: Description and qualification study at meso-β-scale). EERM internal note. No168.(*)

Clapp, R. B., and G. M. Hornberger, 1978: Empirical equations for some soil hydraulic properties. *Water Resour. Res.,* **14,** 601–604.

CLIMAP Project Members, 1981: Seasonal reconstructions of the earth's surface at the last Glacial Maximum. Geol. Soc. Amer., Map and Chart Series, MC-36, 17 pp. + microfiche.

Cosby, B. J., G. M. Hornberger, R. B. Clapp and T. R. Ginn, 1984: A statistical exploration of the relationships of soil moisture characteristics to the physical properties of soils. *Water Resour. Res.,* **20,** 682–690.

Deardorff, J. W., 1977: A parameterization of ground surface moisture content for use in atmospheric prediction models. *J. Appl. Meteor.,* **16,** 1182–1185.

——, 1978: Efficient prediction of ground surface temperature and moisture with inclusion of a layer of vegetation. *J. Geophys. Res.,* **20,** 1889–1903.

Dickinson, R. E., 1984: Modeling evapotranspiration for three dimensional global climate models. *Climate Processes and Climate Sensitivity. Geophys. Monogr.,* **29,** 58–72.

Jackson, R. D., 1973: Diurnal changes in soil water content during drying. *Field Soil Water Regime,* Soil Sci. Soc. of Amer., 37–55.

Jarvis, P. G., 1976: The interpretation of the variations in leaf water potential and stomatal conductance found in canopies in the field. *Phil. Trans. Roy. Soc. London,* **B273,** 593–610.

Mahfouf, J. F., E. Richard and P. Mascart, 1987: The influence of soil and vegetation on the development of mesoscale circulations. *J. Climate Appl. Meteor.,* **26,** 1483–1495.

Mahrt, L., 1987: Grid-averaged surface fluxes. *Mon. Wea. Rev.,* **115,** 1550–1560.

Matthews, R., 1983: Global vegetation and land use: New high-resolution data bases for climate studies. *J. Climate Appl. Meteor.,* **22,** 474–487.

McCumber, M. C., 1980: A numerical simulation of the influence of heat and moisture fluxes upon mesoscale circulations. Rep. UVA-ENV SCI-MESO-1980-2, Dept. of Environmental Science, University of Virginia, 255 pp.

——, and R. A. Pielke, 1981: Simulation of the effects of surface fluxes of heat and moisture in a mesoscale numerical model. Part I: Soil layer. *J. Geophys. Res.,* **86,** 9929–9938.

Mercusot, C., P. Bougeault and Y. Durand, 1986: Atlas des analyses Peridot. Programme HAPEX-MOBILHY (A quiklook of the Peridot analyses during HAPEX-MOBILHY). EERM internal note. (*)

Mintz, Y., 1981: The sensitivity of numerically simulated climates to land surface boundary conditions. *Proc. JSC Study Conf. on Land Surface Processes in Atmospheric GCM,* Greenbelt.

Monteith, J. L., 1975: *Vegetation and the Atmosphere. Vol. 1: Principles.* Academic Press, 278 pp.

——, 1976: *Vegetation and the Atmosphere. Vol. 2: Case Studies.* Academic Press, 439 pp.

Noilhan, J., 1987: Une modélisation unidimensionnelle des échanges énergétiques dans le sol, la végétation et la couche limite atmosphérique (A one-dimensional model for mass and heat exchanges within the soil, the vegetation and the atmospheric boundary layer). EERM internal note. No171.(*)

Ookouchi, Y., M. Segal, R. C. Kessler and R. A. Pielke, 1984: Evaluation of soil moisture effects of the generation and modification of mesoscale circulations. *Mon. Wea. Rev.,* **112,** 2281–2292.

Phulpin, T., and J. P. Jullien, 1987: Characterization of the vegetation with AVHRR data during HAPEX-MOBILHY experiment. E.G.S. XIIx Assembly. *Terra Cognita,* **7,** 523.

Rowntree, P. R., 1983: Sensitivity of GCM to land surface processes. *Proc. Work. in Intercomparison of Large Scale Models for Extended Range Forecasts,* ECMWF, Reading, England, 225–261.

Sellers, P. J., Y. Mintz, Y. C. Sud and A. Dalcher, 1986: The design of a Simple Biosphere model (SiB) for use within general circulation models. *J. Atmos. Sci.,* **43,** 505–531.

Szeicz, G., and I. F. Long, 1969: Surface resistance of crop canopies. *Water Resour. Res.,* **5,** 622–633.

Thompson, N., Barrie and M. Ayles, 1981: The Meteorological Office Rainfall and Evaporation Calculation System: MORECS. *Hydrological Memorendum,* **45,** 69 pp.

Tucker, C. J., and P. J. Sellers, 1986: Satellite remote sensing of primary production. *Int. J. Remote Sens.,* **7,** 1395–1416.

Wetzel, P. J., and J. T. Chang, 1988: Evapotranspiration from nonuniform surfaces: A first approach for short term numerical weather prediction. *Mon. Wea. Rev.,* **116,** 600–621.

Wilson, M. F., and A. Henderson-Sellers, 1985: Cover and soils datasets for use in general circulation climate models. *J. Climatol.,* **5,** 119–143.

* All EERM Internal Notes are available from CNRM, 42, av. Coriolis, 31057 Toulouse Cedex France.